Construction and Building Materials 282 (2021) 122634

Contents lists available at ScienceDirect

Construction and Building Materials

journal homepage: www.elsevier.com/locate/conbuildmat

Experimental and numerical investigation of carbon textile/cementitious matrix interfacebehaviourfrom pull-out tests

Manh Tien Tran [a], Xuan Hong Vu [b,*], Emmanuel Ferrier [b]

[a] Department of Mechanisms of Materials, Hanoi University of Mining and Geology (HUMG), n°18, Pho Vien street, Duc Thang Ward, Bac Tu Liem District, Ha Noi City, Viet Nam
[b] Université de LYON, Université Claude Bernard LYON 1, Laboratoire des Matériaux Composites pour la Construction LMC2, France

HIGHLIGHTS

- Characterization of carbon textile/cementitious matrix interface behaviour by pull-out tests.
- The embedded length affected the pull-out behaviour and total pull-out energy of interface specimens.
- Numerical modeling by using a nonlinear spring model for textile/matrix interface behaviour.
- Numerical modeling by using cracking modeling of the matrix with the concrete material model.
- The numerical modeling gave a reasonable result in comparison with that of the experiment.

GRAPHICAL ABSTRACT

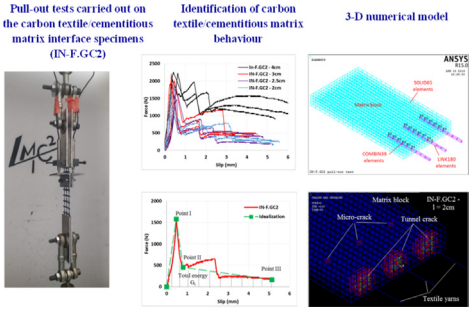

ARTICLE INFO

Article history:
Received 13 October 2020
Received in revised form 4 February 2021
Accepted 7 February 2021

Keywords:
Textile – reinforced concrete (TRC)
Textile/matrix interface
Pull-out test
Embedded length
Element finite model

ABSTRACT

In the context of the application of textile-reinforced concrete composite (TRC) for strengthening or reinforcing of structural elements, an important factor that significantly influences its mechanical behaviour is the bond strength of the textile/cementitious matrix interface. In order to improve this bond, reinforcement textile is usually treated with different products in the manufacturing procedure. This paper presents the experimental and numerical results concerning the mechanical behaviour of carbon textile/cementitious matrix interface from the pull-out tests. The carbon textile was treated with an amorphous silica product to improve the bond with the cementitious matrix and embedded in the cementitious matrix with different lengths. The experimental results showed that all pull-out tests gave typical "force – slip" curves of interface behaviour as shown in the literature with three phases: perfect bonding phase, debonding phase, and pure friction phase. The effects of carbon textile and embedded length on pull-out behaviour and failure mode of textile/matrix interface specimens could be found and analyzed. Concerning the mesoscale modeling work, the numerical model was developed and validated by using a nonlinear spring model for interface behaviour and taking into account the crack damage of the cementitious matrix in the calculation. The numerical results highlighted that the numerical model could predict the relationship of pull-out force and slip for all cases of the embedded length of carbon textiles within the cementitious matrix. This paper shows that both experimental and numerical results on the carbon textile/cementitious matrix interface has a good agreement in pull-out behaviour and failure mode.

* Corresponding author.
E-mail addresses: tranmanhtien@humg.edu.vn (M.T. Tran), Xuan-Hong.Vu@univ-lyon1.fr (X.H. Vu), emmanuel.ferrier@univ-lyon1.fr (E. Ferrier).

https://doi.org/10.1016/j.conbuildmat.2021.122634
0950-0618/

1. Introduction

The industrial textile has been increasingly and widely produced in the factory for the applications in civil engineering. Its combination with a polymer matrix or cementitious matrix forms a new material [Fibre Reinforced Polymer (FRP) or Textile Reinforced Concrete (TRC)] that has better characteristics (high strength and stiffness, lightness, etc) than other traditional materials [1–3]. They have been successfully used for the strengthening or reinforcing of structural elements of existing construction works (old buildings, old tunnels, etc.) or a constituent element of new structures [2–5]. Among these composite materials, TRC composite has preeminent advantages in special environmentssuch ascorrosion, aging, and elevated temperature [2,6].

Over the past decades, the mechanical behaviour of TRC composite has been characterized clearly from the tensile or flexural test in the literature [7–10]. It is a hardening behaviour with three distinguished phases and depending on several factors such as textile nature, matrix nature, reinforcement ratio, etc [11–14]. An important factor that significantly influences the mechanical behaviour of carbon TRC is the bond strength of the textile/matrix interface. A good interface adhesion can improve the work capacity of TRC composite, especially in the first and second phases of its mechanical behaviour [15,16]. Hence, the reinforcement textile is usually treated with different products in manufacturing procedure in order to improve this bond. Furthermore, the bond strength and mechanical behaviour of the textile/matrix interface become an interesting topic to study. Among the methods in the literature for characterizing the response of fibre/matrix interface behaviour, the pull-out test is simple yet efficient in laboratory conditions [17]. The following paragraphs present the previous research which focuses on the experimental and numerical behaviour of the interface between fibre (different fibre types) and the cementitious matrix from the pull-out test. The objective of this study is presented at the end of the introduction of this paper.

1.1. Previous experimental studies of interface behaviour from pull-out tests

Until now, there have been several studies on the behaviour of fibre/cementitious matrix interface from the pull-out tests [6,18–22]. Ferreira et al. [20] have carried out the pull-out tests on interface specimens to identify the nature of fibres/matrix bond in cement-based systems. In this study, the influence of natural fibres characteristics on the interface mechanics with cement-based matrices was found. Silva et al. [23] have performed the double-sided pull-out test on interface specimens between carbon fibres and finely grained concrete matrix after being preheated at different temperatures in order to find the elevated temperature effect on the interface properties. The durability effect on the alkali-resistant glass fibre/-matrix interface was investigated from the double-sided pull-out test at different ages of the cementitious matrix [24]. Fidelis et al. [25] have conducted on the effect of accelerated aging on the interface of jute textile-reinforced concrete. Homoro et al. [18] have recently studied the pull-out response of alkali-resistant (AR) glass yarn from the ettringite matrix with the different pre-impregnation methods and embedded lengths. The effect of fibre treatments on the sisal fibre/matrix bond strength in cement-based systems from the pull-out test was investigated by Ferreira et al. [26]. Lu et al. [27] have studied the improvement of interfacial bond strength of carbon fibre in the cementitious matrix with a thin SiO_2 layer coating. The pull-out tests of glass multi-filament yarn embedding in a cementitious matrix with different lengths were carried out for analyzing its failure mechanism and to find a fracture mechanism of an analytical model for interfacial behaviour [28].

All available results in the literature shows a softening behaviour of fibre/matrix interface from the pull-out test with three phases: phase of the perfect bond, phase of debonding, and phase of pure friction [17,29]. However, depending on the test configuration, the fibre/matrix interface specimen had differently response types from the pull-out test [30]. Moreover, bond strength and mechanical behaviour of fibre/matrix interface depended greatly on several factors from studied fibre and matrix, such as nature, treatment product, geometry of fibre, matrix nature [18,20,22,23,26,27,31,32], and environment conditions such as elevated temperature, aging condition [23–25].

Concerning the effect of fibre treatment on fibre/matrix interface response from the pull-out test, it could be found clearly this scientific point in a few research works in the literature. According to Ferreira et al. [26], sisal fibres were treated with different treatment methods: hornification method, alkali and hybrid treatment, and polymer impregnation. The results of the pull-out tests showed that, by comparing with the specimens of natural sisal fibres, a significant improvement in the fibre/matrix interface bond has been verified. With the polymer treatment, it could be found a better frictional mechanism and a slip-hardening behaviour of the fibre–matrix bond. With the alkali treatment, the amorphous constituents of the fibre were removed from the fibre surface to increase the roughness of sisal fibres, while the hornification phenomena improved the bond strength of sisal fibre–matrix thanks to the stiffening of the polymeric structure of the fibre-cells. In the experimental study of Homoro et al. [18], in order to improve the interfacial bond between AR glass yarn and ettringite matrix, fibres were treated with different products by dry and wet pre-impregnated methods. In conclusion, for carbon fibre, there were many effective treatment products to improve its interfacial bond strength with the cementitious matrix. In the research of Lu et al. [27], the authors successfully used nano-SiO_2 as a coated layer in order to improve the interfacial properties of carbon fibre and cementitious matrix. With this treatment by SiO_2, the interfacial adherent was improved thanks to the appearance of C-S-H gel at the interface which was the product of the chemical reaction between SiO_2 and cement hydration product $Ca(OH)_2$. This chemical adhesion enhancement improved the bond strength, frictional bond strength, and chemical debonding energy to approximately 3, 2, and 10 times of that of non-treated carbon fibre specimens, respectively.

Concerning the effect of embedded length, theoretically, the longer embedded length would give more fiber/matrix interface surface for adhesion between both materials. Therefore, the maximum pull-out force would be normally increased almost linearly depending on the embedded length. In fact, with such length, there is possibly an appearance of the damage phenomena on the interface surface or on the cementitious matrix during the tests, which could strongly affect the results obtained from pull-out tests. In the work of Ferreira et al. [26], the sisal fibre has been embedded in Portland cement-based matrix with different lengths (5, 10, 25, and 50 mm), and the embedment lengths gave different results in pull-out response. According to the results obtained by previous studies [18,21], the maximum pull-out force was increased with the extension of embedded length. However, if the embedment length was too long, fibre damage would probably occur before the total debonding [18,21]. So, the results obtained were not exactly the behaviour of the fibre/matrix interface.

1.2. Previous numerical studies for textile/matrix interface behaviour

In the literature, several numerical or analytical studies aimed to characterize the behaviour of the interface between textile (or fibre)/matrix in TRC composite or in composite strengthening

systems. Regarding the analytical approach, these models have been constructed to explain the failure mechanisms of the textile/-matrix interface. Some researches studied analytically the bond behaviour of Fabric-Reinforced Cementitious Matrix (FRCM) strengthening systems [15,33–35]. Carozzi et al. [35] have proposed a cohesive interface crack model for the matrix–textile debonding in FRCM composites. Grande and Milani [33] have studied an effective spring model by considering the effect of matrix damage on the shear behaviour at the fibre/mortar interface in FRCM strengthening systems. Zhang et al. [21] have developed an analytical model for pull-out specimens of glass fibre (E and AR) embedded in a block of the cementitious matrix. As numerical results, it could be found that analytical modeling was usually based on the approach of the rupture mechanism. The shear failure of the interface between the textile yarn and the cementitious matrix was considered as the criteria of a tunnel crack at the interface. Regarding the numerical approach, several studies have been conducted on the textile/matrix interface specimens at the material scale or at the structural scale [33,36,37]. Mazzucco et al. [38] have developed a finite element model of the bond behaviour of FRCM composites by using a mesoscale approach. Djamai et al. [36] have studied numerically at microscale the bond-slip behaviour of textile reinforced concrete in application to TRC sandwich panels. These numerical models have considered a non-linear-elastic behaviour of the cementitious matrix layers (mortar or concrete), as well as a non-linear bond-slip behaviour of the interfaces interposed between the textile and matrix layers. The results obtained from these numerical models showed a good agreement with that of the experimentand analytical model.

According to Teklal et al. [17], the interface debonding condition was defined by two distinct approaches: the shear strength criteria and the failure mechanism approach. In the approach of the criteria of shear strength, when the shear stress at the interface reached the resistance at limit state, the debonding occurred at the interface between two components. Concerning the failure mechanism approach, the extension of a debonding crack required that the potential energy release portion of the composite components reached a critical value (called the interface fracture toughness). Both numerical and analytical models based on these approaches gave a good agreement with experimental results in the literature.

1.3. Objective of this study

To the best of the authors' knowledge, no results concerning pull-out tests carried out on carbon textile/cementitious matrix interface specimens are available. There are also not yet numerical results regarding the element finite (EF) model for pull-out tests of interface specimen of carbon textile and cementitious matrix. So, in order to understand the textile/matrix interface behaviour in TRC composite, this study aimed to characterize the pull-out behaviour with both experimental and numerical approaches. This paper also contributed additionally to the knowledge about the mechanical behaviour of the textile/matrix interface. The carbon textile used in this study was a commercial product with the treatment of an amorphous silica product and was embedded in a concrete matrix with different lengths. The pull-out specimens were tested by using the tensile machine and measurement chain with Linear Variable Differential Transducer (LVDT) for a bond-slip of the interface. Thanks to this test configuration, the "force – slip" curves could be drawn from pull-out tests. After that, a numerical model was developed and validated using a spring model for interface behaviour and taking into account the cracking of the cementitious matrix. The experimental and numerical results obtained were compared together and discussed in this study.

2. Experimental works

This section respectively presents the equipment used, the material used and interface specimens, test procedure, a summary of specimens and tests.

2.1. Equipment used

2.1.1. Test machine

The test machine, used for the pull-out tests, has a high force capacity up to 65 kN for the direct tensile or compressive test. This machine is also well equipped with a measurement chain that can be connected to measurement instruments (with contact measurement methods such as strain gauge or LVDT) to measure deformation or relative displacement between two points of the specimen (see Fig. 1). The tensile load was controlled by the vertical movement of the traverse thanks to the controlling program in the system computer (see Fig. 1b). During the test, the data, including the mechanical load and the transverse movement of the test machine, were recorded at least twice per second and could then be exported in the form of datasheets for the result analysis. Fig. 1 below presents the test machine with other equipment for pull-out tests.

2.1.2. Lvdt

The LVDTs were used for pull-out tests to measure the relative slip between two measurement points in carbon textile and cementitious matrix plate when the tensile force increased with time. Two LVDTs were fixed on two surfaces of aluminum plates by a mechanical system. Another system was also fixed on the carbon textile at the position next to the matrix plate. This configuration ensured the negligible deformation of the carbon textile between two mechanical systems. Therefore, the displacement obtained from the LVDTs was a bond-slip of pull-out tests. Fig. 2 shows the LVDTs configuration for pull-out tests.

2.2. Material used and interface specimens

This section presents the cementitious matrix and carbon textiles studied and the preparation of textile/matrix interface specimens for pull-out tests in this study.

2.2.1. Cementitious matrix

The cementitious matrix used in this experimental study was designed with a laboratory condition to produce carbon TRC specimens as in the authors' previous study [39]. This matrix consisted of the silico-aluminous-calcic synthetic aggregate, containing about 40% of alumina, obtained by melting, and was characterized by a high density and exceptional hardness in addition to cement that essentially consisted of calcium aluminates constituting a binder for refractory applications. The high mono-calcium aluminate content of this cement (about 50%) gave the concrete good mechanical performance. For a small thickness of the application, the maximum diameter of the aggregate should be less than 1.25 mm. In particular, a small amount of super-plasticizer and viscosity modifier has been added to the concrete component. The water/cement ratio of this cementitious matrix was 0.35. The mechanical properties of the cementitious matrix were characterized by compression tests according to the European standard BS EN 196-1 [40] and tensile tests in the authors' previous study [39]. Table 1 below presents the mechanical properties of the cementitious matrix at 28 days.

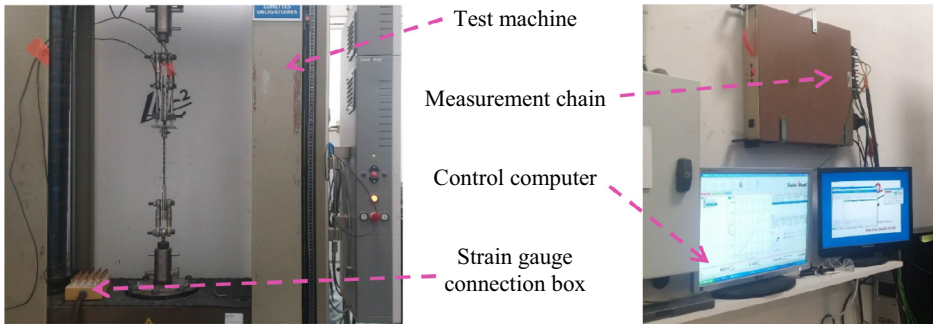

Fig. 1. Test machine for experimental works; (a) General view of the pull-out test configuration; (b) Control system of the test.

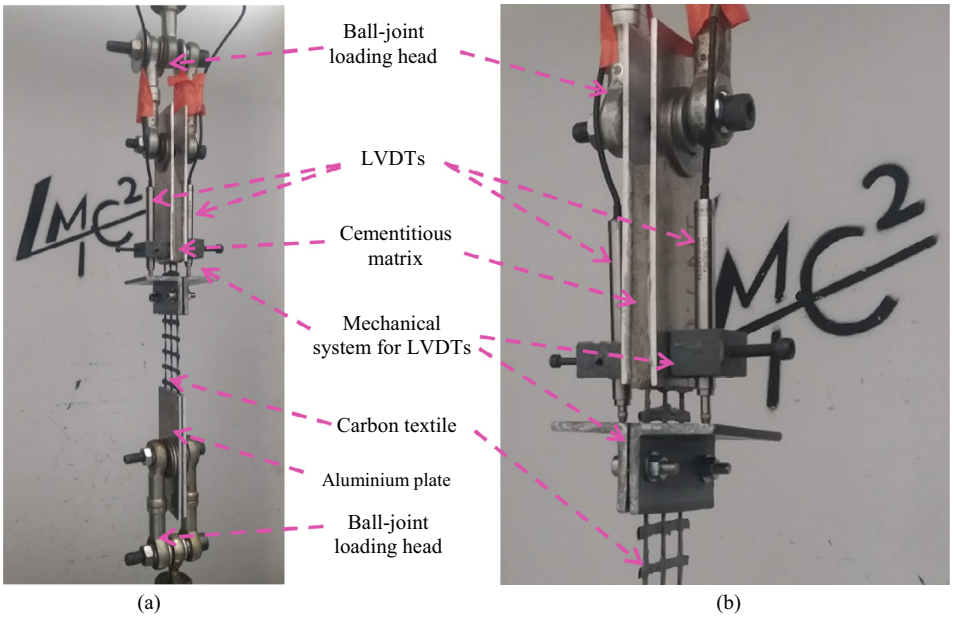

Fig. 2. Pull-out test setup; (a): Overview of LVDT configuration; (b) Detail of LVDT set-up.

Table 1
Mechanical properties of the cementitious matrix at 28 days [39,40].

Mechanical properties of the cementitious matrix	Average value	Standard deviation
Compressive strength at 28 days (BS EN 196-1, 2005)	58.1 MPa	2.5 MPa
Tensile strength	5.29 MPa	0.11 MPa
Young's modulus	8.41 GPa	1.14 GPa

2.2.2. Reinforcement textiles

The continuous carbon textile used (called GC2 – Grid of Carbon fibre 2) in this experiment was industrial products that were manufactured in a factory in grid form. The geometry of the carbon grid in the longitudinal and transverse directions was 17 mm × 17 mm (see Fig. 3a). The cross-section of wire (the warp as well as the weft) was 1.795 mm^2. This textile had some advantages, such as very high tensile strength and Young's modulus, high corrosion resistance, low weight per unit area, simple and flexible application. Furthermore, it was treated with an amorphous silica product to improve bond adherence with the cementitious matrix (see Fig. 3b). The mechanical capacities of this carbon textile were identified in the authors' previous research [39,41]. The mechanical properties of the GC2 carbon textile are summarized in Table 2.

2.2.3. Specimen preparation

The GC2 carbon textile/cementitious matrix interface specimens were fabricated in the laboratory condition for pull-out tests (called IN-F.GC2 in this study). The preparation of pull-out specimens was performed using hand lay-up technique in the following procedure. Firstly, the cementitious matrix was prepared with its formulation as in the authors' previous research [39] (see Fig. 4a). Afterwards, the rectangular plates of a cementitious matrix with dimensions of 100 mm × 300 mm × 10 mm (length × width × thickness) were moulded with different embedded lengths of GC2 carbon textiles in it. The embedded length varied from 2 cm to 4 cm for IN-F.GC2 specimens. The placement of GC2 carbon textile was established in the same way for all cases of embedded length in the matrix block of pull-out specimens. A transversal yarn (the weft) was placed at the border of the cementitious matrix plate, and the carbon textile part anchoring in the cementitious matrix block was extended until the reaching of the embedded length. Then, after curing of the cementitious matrix (28 days), each specimen plate was cut (the matrix as well as the carbon textile), to obtain the specimens with the cementitious matrix block dimensions of 100 mm × 51 mm × 10 mm (length × width × thickness) (see Fig. 4b). Both ends of the test specimens were bonded with aluminium plates to transfer tensile load on the pull-out test specimens (see Fig. 4c). Finally, all sam-

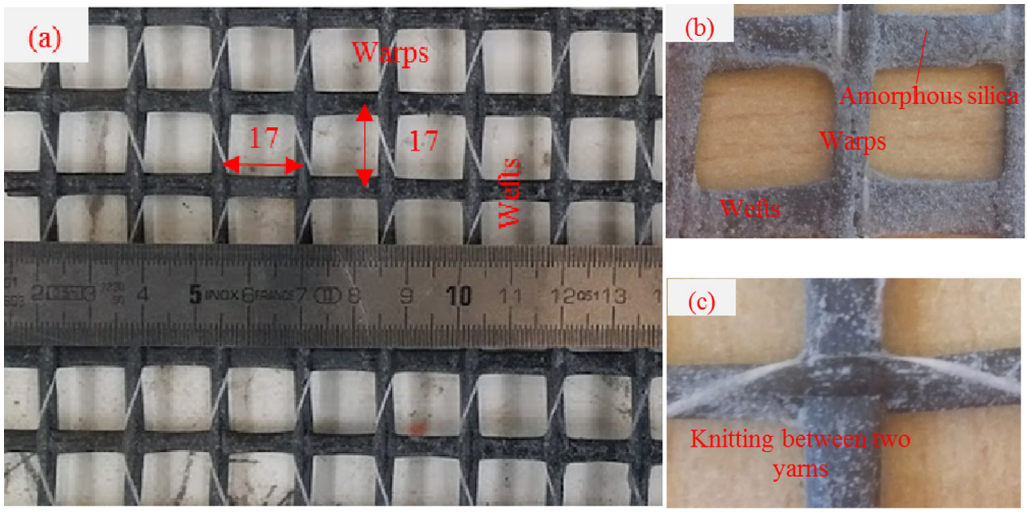

Fig. 3. Carbon textile used in the experimental study; (a) Carbon grid geometry (dimension in mm); (b) Treatment product on carbon textile; (c) Detail of knitting between the warp and weft.

Table 2
Mechanical and physical properties of the studied carbon textiles [39,41].

Properties	GC2
Ultimate strength (MPa)	1312
Young's modulus (GPa)	144
Ultimate strain (%)	0.97

ples were labeled for the tests (see Fig. 4d). Fig. 4 below shows the preparation procedure of pull-out test specimens IN-F.GC2.

2.3. Summary of specimens and tests

Table 3 shows the list of specimens for the pull-out tests in this experiment. There were 12 tests carried out on the interfacial specimens of GC2 carbon textile embedded in matrix plates with different lengths, from 2 cm to 4 cm.

3. Experimental resultsand discussion

This section presents all results of pull-out tests performed on carbon textile/cementitious matrix interface specimens (IN-F.GC2), including the pull-out behaviour, the failure modes, and the pull-out energy of interface specimens.

3.1. Pull-out test results

3.1.1. Pull-out behaviour of IN-F.GC2 specimens

Fig. 5a presents all force-slip curves obtained from pull-out tests performed on IN-F.GC2 specimens with different embedded

(a) Preparation step of the cementitious matrix

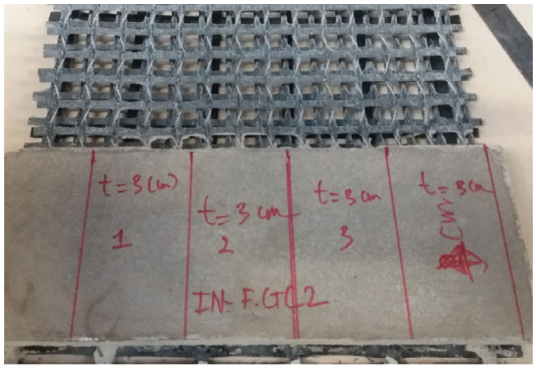

(b) Molding of the specimen plate (IN-F.GC1)

(c) Bonding with aluminum plates

(c) Labeling of the pull-out test specimens (IN-F.GC2)

Fig. 4. Preparation procedure of pull-out test specimens.

Table 3
List of tests carried out on the pull-out specimens; (a, b, c: names of different tests carried out in the same condition).

Specimens	Dimensions of matrix block [length × width × thickness (mm^3)]	Embedded length (mm)	Number of tests
IN-F.GC2 – 2 cm (a,b,c)	100 × 51 × 10	20	3
IN-F.GC2 – 2.5 cm (a,b,c)		25	3
IN-F.GC2 – 3 cm (a,b,c)		30	3
IN-F.GC2 – 4 cm (a,b,c)		40	3
Total of tests			12

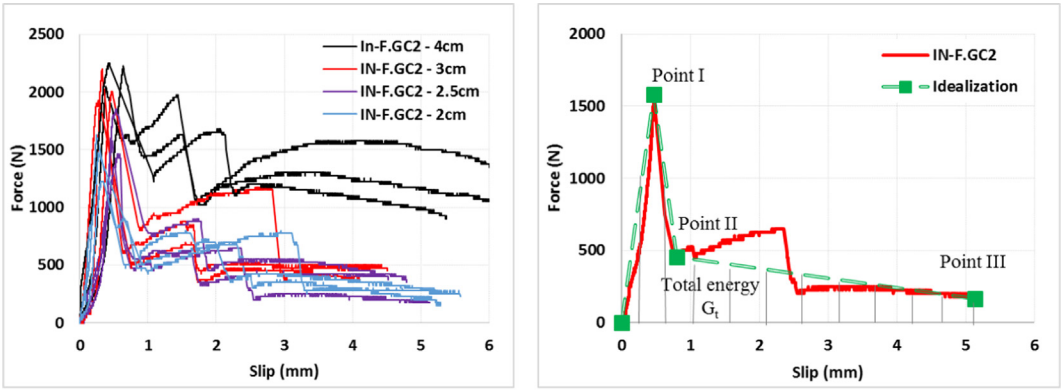

Fig. 5. Experimental results of pull-out tests; (a) All "force – slip" curves of IN-F.GC2; (b) Idealization of the pull-out behaviour.

lengths. Regarding results, it was found that the pull-out specimens gave the softening behaviour for the textile/matrix bond with three phases as presented in the literature [17]. The first phase was the perfect bonding one from the beginning point into the top point in which the "force – slip" relationship is almost linear. The second phase is called the debonding one which was characterized by a significant drop in the pull-out force after reaching the maximum value. The final phase was called the pure friction one which could be drawn par the progressive decrease of pull-out force with the increase of slip between the cementitious matrix block and carbon textile. At the beginning of this phase, the force-slip curve showed a queue form with a slight rise of the pull-out force and then a slight drop in this one.

In order to characterize the pull-out behaviour for IN-F.GC2 specimens, an idealization curve was drawn by using the notation for the typical points (see Fig. 6b) as detailed below:

Point 0 defines the beginning of the "pull-out force – slip" curve.

Point I defines the end of the perfect bonding phase and the beginning of the debonding phase; it is the top of this curve, and the force corresponding with this point is called the maximum pull-out force.

Point II defines the end of the debonding phase and the beginning of the pure friction phase; the slip value in this point corresponds with that of the point after the first drop while the force value is calculated to ensure the similar values of total energy.

Point III defines the end of the pure friction phase and the end of the "pull-out force-slip" curve.

With an idealization presented above, the pull-out behaviour could be drawn for all interface specimens with different embedded lengths. Fig. 6 presents all "force-slip" curves and the average one for 4 cases of embedded lengths from 2 cm to 4 cm. Regarding results, it could be found that the maximum pull-out force generally increased with the extension of this length. The same tendency could be observed for the relation between the force in the pure friction phase and embedded length. Table 4 below shows all values (force and slip) of the typical points of pull-out behaviour, as well as the average pull-out force per unit of embedded length (F_{ave}) for IN-F.GC2 specimens with different cases.

3.1.2. Total energy

The total energy of pull-out work is the energy necessary to damage the textile/matrix bond at the interface. It is not included the deformation energies which were accumulated in carbon textile yarns and matrix block. Generally, this energy could be calculated from the bond-slip curve of the pull-out behaviour of textile/matrix interface specimens. In the case of this study, it was identified as the area limited by the "force-slip" curve of its behaviour as presented in Fig. 5b.

As experimental results concerning the total energy for pull-out work of IN-F.GC2 specimens, it could be found that there was a progressive increase of this value with the embedded lengths from 2 cm to 3 cm. When the embedded length extends from 3 cm to 4 cm, the total energy of IN-F.GC2 specimen significantly increases from 1.86 times to about 4.76 times compared with its value of IN-F.GC2 – 2 cm. This result could be explained by the effect of embedded length on the pull-out behaviour of IN-F.GC2. Due to the embedded length of 4 cm, this specimen maintained a great force in the pure friction phase of its response which gave a value that was considerably higher than that of other specimens.

3.1.3. Failure mode

The textile/cementitious matrix interface specimens were observed after pull-out tests to analyze the failure mode. All IN-F.GC2 specimens showed just only failure mode par the pull-out of carbon textile from the cementitious matrix block. This interface failure occurred progressively with the cracking of the cementitious matrix around the position of carbon textile warps. So, it could be said that all pull-out specimens presented a failure mode par rupture at the textile/matrix interface. Basically, the process of this rupture included the inelastic and dissipative mechanisms of

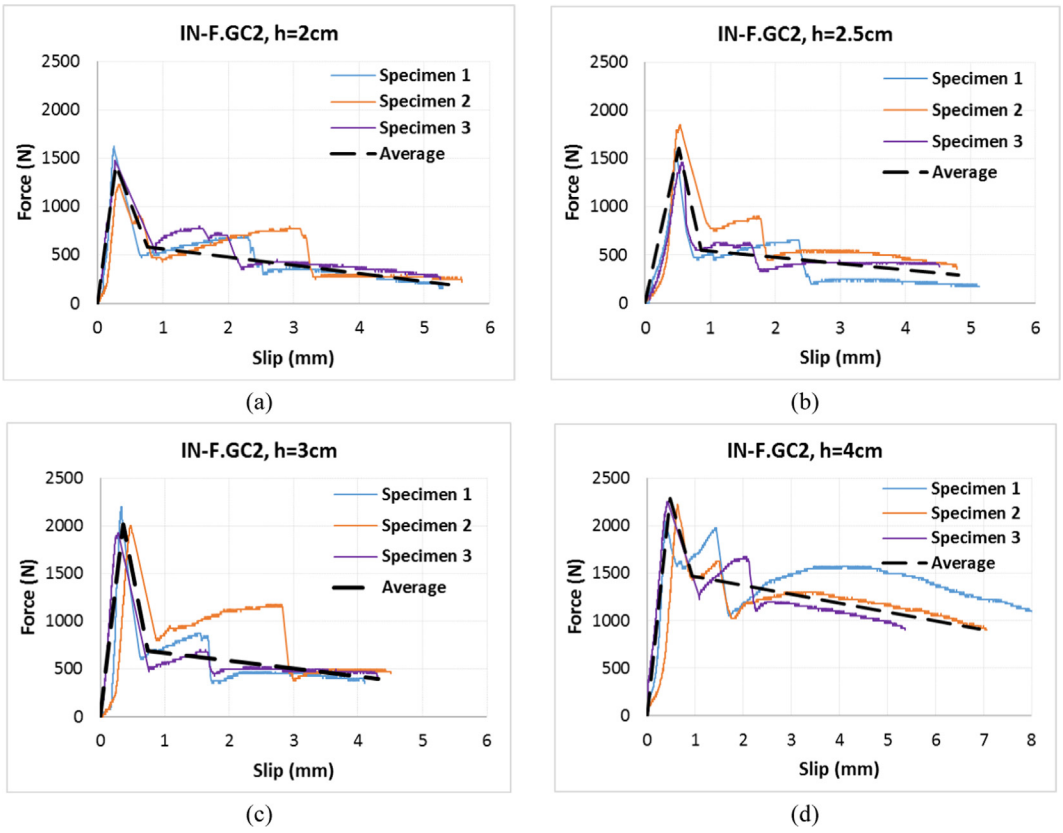

Fig. 6. "Force-slip" curves of the IN-F.GC2 specimens with different embedded lengths.

Table 4
Experimental results obtained from pull-out tests on IN-F.GC2 samples with different embedded lengths (2 cm, 2.5 cm, 3 cm and 4 cm); F_{ave} : average pull-out force per unit of embedded length; G_t : total energy.

Specimens	Point I		Point II		Point III		G_t	F_{ave}
	Force (N)	Slip (mm)	Force (N)	Slip (mm)	Force (N)	Slip (mm)	(N.mm)	(N/mm)
IN-F.GC2 – 2 cm (a,b,c)	1429.79 (196.55)	0.281 (0.037)	579.89 (16.32)	0.761 (0.115)	198.87 (35.95)	5.367 (0.184)	1554.06 (104.34)	71.49 (9.83)
IN-F.GC2 – 2.5 cm (a,b,c)	1609.71 (211.57)	0.519 (0.042)	549.20 (106.40)	0.865 (0.166)	295.50 (114.90)	4.813 (0.306)	2018.28 (458.71)	64.39 (8.46)
IN-F.GC2 – 3 cm (a,b,c)	2015.26 (163.29)	0.359 (0.098)	686.34 (183.71)	0.736 (0.121)	393.83 (63.89)	4.308 (0.204)	2889.99 (486.85)	67.18 (5.44)
IN-F.GC2 – 4 cm (a,b,c)	2288.28 (127.62)	0.485 (0.135)	1473.06 (161.79)	0.943 (0.165)	913.36 (75.85)	6.915 (1.476)	7399.15 (584.77)	57.21 (3.10)

the textile/matrix interface. So, the residual capacity of the textile/-matrix interface after the major debonding decreased progressively with the increase of the slip between textile warps and cementitious matrix. In the pull-out force-slip curve, this failure mode corresponded with the pure friction phase of its behaviour.

After pull-out tests, it could be observed on the IN-F.GC2 specimens that a matrix part was pulled out from the matrix block with carbon textile (see Fig. 7a). This presented the matrix valleys around each textile yarn of the sample (see Fig. 7b). Furthermore, we could also observe the cracks under the tunnel form at the warp positions. These cracks were caused by the load transfer from the tensile force in carbon textile to the matrix block. The part of the warps pulling out from the matrix was coated with a thin layer of the matrix, which was the product of the reaction between the amorphous silica treatment and cement paste [27].

3.2. Discussion

This section presents the discussions to explain the effects of carbon textile and embedded lengths on the results obtained (pull-out behaviour, maximum pull-out force, total energy and failure mode of interface specimens), which were presented in Section 3.1.

3.2.1. Effect of carbon textile on pull-out behaviour

As experimental results obtained, IN-F.GC2 specimens gave a softening behaviour with three distinguishable phases for all embedded lengths, as presented in Fig. 6. This pull-out response was affected by the physical characteristics of GC2 carbon textile. Firstly, its geometry had significant influence on the interaction between textile and matrix in the case of pull-out tests. With the presence of the transversal yarns (the wefts) in the matrix block, it greatly contributed to hold back the carbon textile against the pull-out force. The wefts could be considered as nonlinear spring to connect the longitudinal yarns (the warps) with the matrix block in this case. The failure mechanism of the textile/matrix interface gradually occurred from outside to inside along the embedded length. Each drop of force on pull-out behaviour corresponded with the debonding at the position of transversal yarn. In the last phase, the knitting between the warps and the wefts

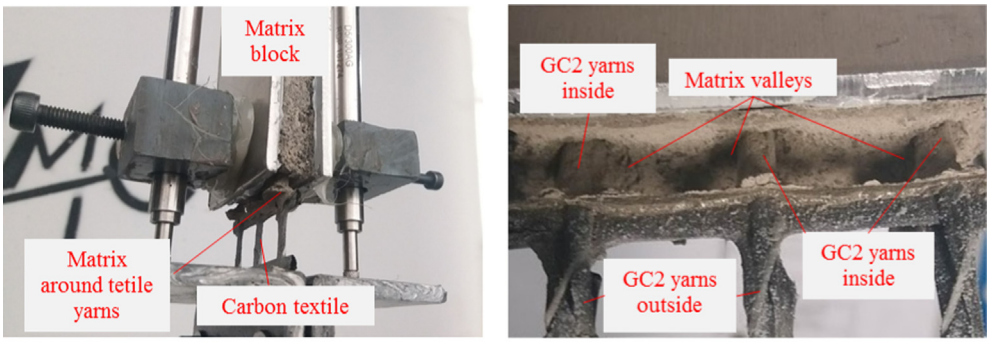

Fig. 7. Failure modes of interface specimens after pull-out tests; (a) During the test; (b) after the test.

helped the carbon textile not to be slipped out from the matrix block. Hence we could observe a progressive failure characterized by a gradual decrease of pull-out force as a function of slip.

Secondly, the textile treatment has also affected the failure mechanism of the longitudinal yarns/matrix interface. The textile warps were formed by approximately 3200 monofilaments (2×1600 tex/strand) with a treatment product of amorphous silica. This product can react with the cement hydration product $Ca(OH)_2$ to form a C-S-H gel, as demonstrated in the literature [27] (see Fig. 8). This thin layer of C-S-H gel gave a good adhesion between carbon textile yarns and cementitious matrix. When the carbon textile was loaded by the pull-out force, the carbon filaments of the warp moved toward themselves to tighten together. The tightening, in this case, generated the torsional stress around the section of the system between textile yarn and C-S-H gel. This stress component in combination with shear stress in the longitudinal direction damaged the cementitious matrix to generate the crack tunnel along with the yarn/matrix interface (see Fig. 8b). At the outside, the effect of these stress components could be clearly found by the matrix valleys in spiral form on pull-out specimens (see Fig. 8a).

3.2.2. Effect of embedded length on pull-out behaviour

Regarding the effect of embedded length on the pull-out response, it could be found that the maximum pull-out force increased gradually with the rise of this length. Clearly, in order to damage the system including the connection between the warp and weft yarns and embedded zone in the matrix block, it was necessary to generate the relative displacement of carbon textile within the matrix block. So, with the longer embedded length, the necessary pull-out force was higher to give rise to the beginning of tunnel crack around warp yarns. However, this tendency was not linear for all cases of embedded length. In practice, the textile/matrix interface was damaged just only a part of its length from the outside to the position of the next weft yarns. So, the increase of pull-out force was not linear with the embedded length. In the case of IN-F.GC2 specimens with an embedded length of 4 cm, the maximum pull-out force increased slightly compared to that of IN-F.GC2 with 3 cm in embedded length. Concerning the effect of embedded length on pure friction force of pull-out behaviour, an inverse effect could be observed from Fig. 9a. For IN-F.GC2 with 4 cm in embedded length, after being damaged on a part, the interface length was long enough to maintain a greater frictional force in comparison with that of other specimens of the smaller embedded length. On the other hand, IN-F.GC2 specimens with three other embedded lengths (2 cm, 2.5 cm, and 3 cm) gave an almost linear tendency of maximum pull-out force and pure friction force with the increase of embedded length.

The effect of embedded length on the total pull-out energy is shown in Fig. 10b below. According to this figure, a significant increase in this value of IN-F.GC2 specimens could be found with interface specimens of carbon textile embedded 4 cm in the matrix. This result comes from thevery higher friction force in the third phase compared to the other pull-out specimens. In this phase, the energy was consumed to gradually damage the textile/-matrix interface and decrease the pure friction force while the slip increases with time. As a result, the total energy increases from 1554 N.mm for IN-F.GC2 – 2 cm, to 7399 N.mm for IN-F.GC2 – 4 cm.

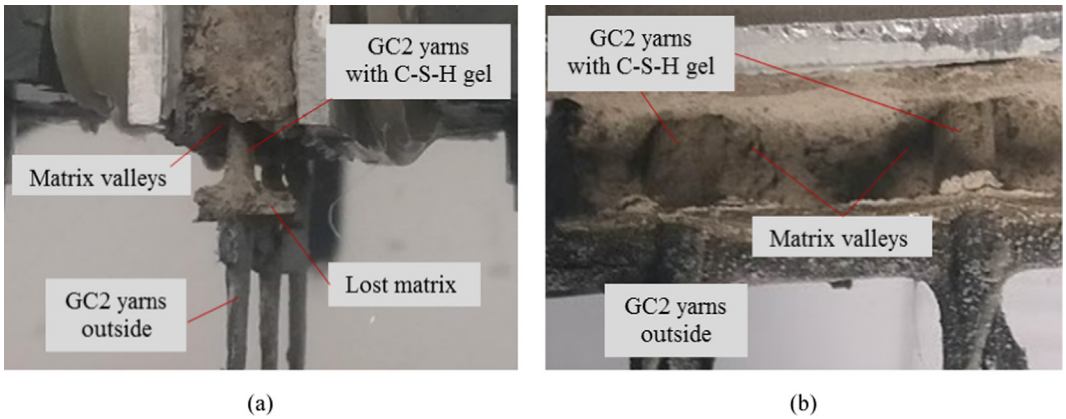

Fig. 8. Effect of textile treatment on the failure mode of pull-out specimens; (a) Damage of cementitious matrix around the warp yarns; (b) Matrix valleys in spiral form.

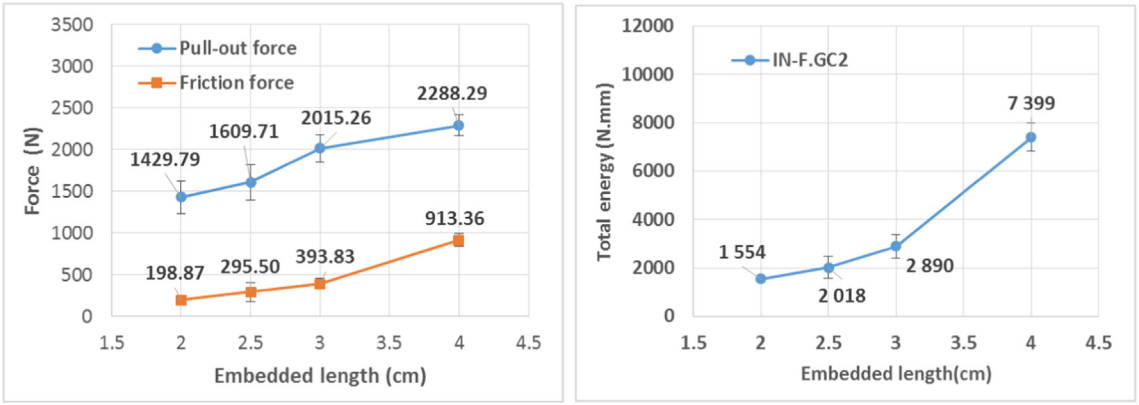

Fig. 9. Effect of embedded length on pull-out behaviour; (a) for pull-out force; (b) for total energy (G_t).

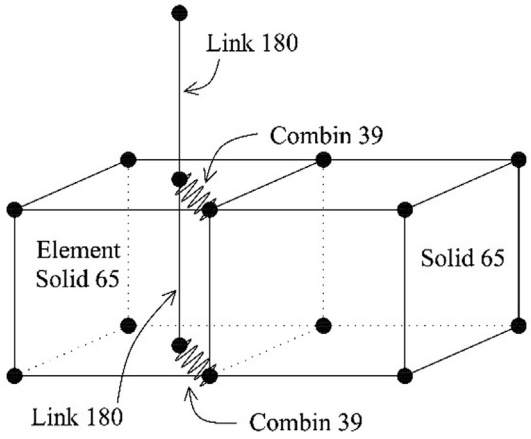

Fig. 10. Configuration of elements used in the numerical model (available in the finite element code [42]).

4. Finite element modeling

This section presents a three-dimensional finite element model for the pull-out specimen in which a tri-linear bond-slip model was used for carbon textile/matrix interface behaviour as well as the damaged concrete behaviour for cementitious matrix. This numerical modeling was developed on account of the finite element code [41].

4.1. Numerical model

The modeling procedure for this model included the type of elements used, the material model, the mesh, the boundary conditions and loads.

4.1.1. Element types

In this numerical model, the used elements were LINK180 (3-D Spar or Truss) for the carbon textile and SOLID65 (3D Reinforced Concrete Solid) for the cementitious matrix. For the interaction between the carbon textile and cementitious matrix, the COMBIN39 element (Nonlinear Spring) was chosen in this numerical model. It was a nonlinear spring to link between two nodes: the SOLID65 element node of the cementitious matrix and the LINK180 element node of the textile (see Fig. 10). The adhesion between two elements (SOLID65 and LINK180) was characterized by the behaviour law of this spring model. When there was the relative displacement (called slip) between two nodes at the interface, this generated a reaction force in the spring element to hold back the textile yarns in the matrix block. Fig. 10 below shows the configuration of the COMBIN39 element in the numerical model of the pull-out specimen.

4.1.2. Material model

This numerical modeling was based on the material models for carbon textile, cementitious matrix, and the interface between both components, in which the material properties were specified for numerical calculation. Firstly, for the behaviour law of carbon textile, the perfect linear elastic model was chosen to simulate its work under the action of mechanical load. The essential parameters of this material model were ultimate strength and Young's modulus which have been obtained from a previous experimental study of the authors [39,43], and presented in Section 2.2.2. Then, the concrete model (CONCR - Nonlinear Behaviour - Concrete) was used for the cementitious matrix in this numerical model. This material model could predict the failure of fragile materials (concrete, stone, ceramics, etc.) in which the failure modes (cracking or crushing) were taken into account for crack modeling. The presence of a crack at an integration point was represented by the modification of the stress–strain relations by introducing a plane of weakness in a direction normal to the face of the crack. Besides, a shear transfer coefficient was introduced, which represented a shear strength reduction factor for subsequent charges that induced slip (shear) on the crack face. Fig. 11a below presents the stress–strain relationship in the coordinate system parallel to the principal stress directions.

For the connection between the textile yarns and the cementitious matrix, the nonlinear combination model (Nonlinear Spring - COMBIN39) [42] was chosen to simulate the interaction between two materials. With this material model, it could explicitly define the force-slip curve for the COMBIN39 element by entering discrete force points as a function of the slip. From the experimental results obtained, the pull-out force - slip relationship could be proposed for the connection between a textile yarn and the cementitious matrix as shown in Fig. 11b.

In order to determine the parameter F_{max} in Fig. 11b, a parametric study of the influence of this value on the pull-out force was carried out. This study was based on the experimental data of IN-F.GC2 with the embedded length of 2 cm. Firstly, the average bond strength of the interface specimen (F_{ave}) was calculated by the ratio between the maximum pull-out force and the embedded length. However, in practice, the interface was not damaged at the same time in 3 textile warps as well as along their length. So, the

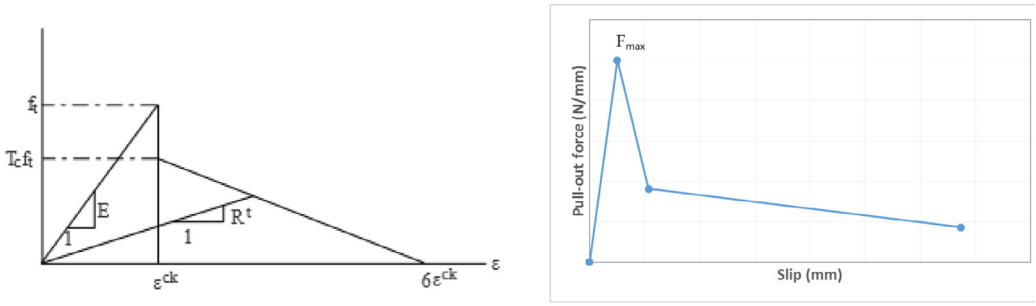

(a) Model for cementitious matrix (b) Model for interface behaviour

Fig. 11. Material models for this numerical modeling; (a): Model for cementitious matrix [42]; (b) Model for interface behaviour.

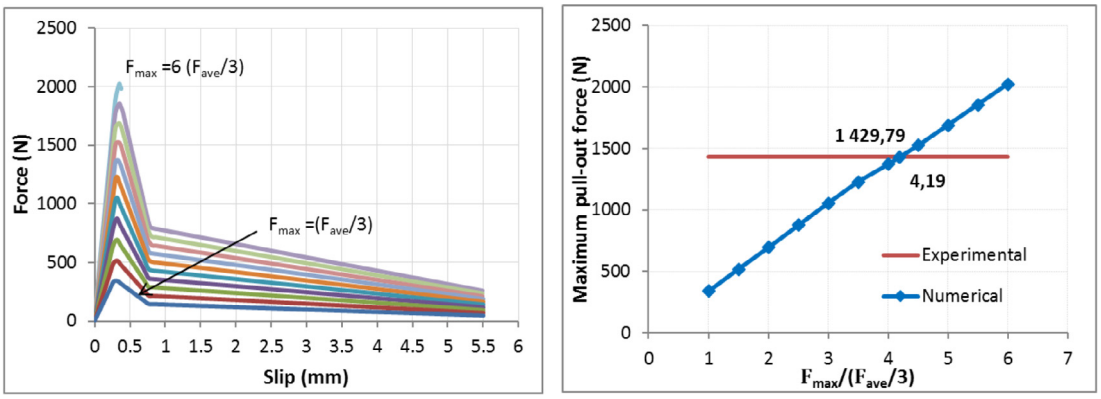

(a) Pull-out behaviour of interface depending on the ratio $F_{max}/(F_{ave}/3)$ (b) Evolution of the maximum pull-out force as a function of the ratio $F_{max}/(F_{ave}/3)$

Fig. 12. Parametric study of the influence of the material model on the pull-out behaviour and maximum pull-out force.

value of F_{max} in the material model of COMBIN39 element was involved from 1 to 6 times of the ratio $(F_{ave}/3)$ (because there were three textile warps for each interface specimen). The result showed that the pull-out behaviour and maximum pull-out force depended on the input data of F_{max} (see Fig. 12). In comparison with the experimental result of IN-F.GC2 – 2 cm, the corresponding value F_{max} was 4.19 times of the ratio $(F_{ave}/3)$ (see Fig. 12b). This meant that the value of F_{max} in the material model of the COMBIN39 element was 99.97 N/mm, and this value was used for all cases of embedded length.

The essential parameters of the numerical model identified thanks to experimental results obtained previously by the authors, are presented in Table 5.

4.1.3. Meshing, boundary conditions and loads

In order to simulate the pull-out work of carbon textile from a matrix block, a specimen model was generated in the same geometry as the experimental one with the dimensions of 100 mm × 51 mm × 10 mm (length × width × thickness) for matrix block. Three GC2 yarns (the warps) were embedded in this matrix block with different lengths from 2 cm to 4 cm. In this numerical model, the effect of transversal yarns (the wefts) on the pull-out force was taken into account in the non-linear spring model of the textile/matrix interface. So, it could not be necessary to add the transversal yarns of textile.

Concerning the mesh of the numerical model, the matrix block and the textile yarns were meshed so that there were common nodes between the cementitious matrix elements (SOLID65) and the textile yarn elements (LINK180). Fig. 13a below presents the mesh of the numerical model for two specimens of the interface IN-F.GC2.

Regarding boundary conditions, all nodes on two surfaces of the matrix block bonded with two aluminum plates in corresponding experimental tests were fixed all displacements (see Fig. 13b). The mechanical loading was applied to the pull-out specimen by the displacements imposed on the ends of three textile yarns. The increasing rate of displacements imposed was controlled by the numerical calculation time. This loading was also divided by steps to more easily observe the pull-out behaviour of the interface model.

4.2. Numerical results

This section presents the results obtained from the numerical model for pull-out specimens with different embedded lengths,

Table 5
Mechanical properties of the materials in the numerical model.

Carbon textile (LINK 180)		Cementitious matrix (SOLID 65)				Interface (COMBIN 39)
σ_f (MPa)	E (GPa)	E (GPa)	f_t (MPa)	ε_{ck}	Tc	F_{max}(N/mm)
1312	143.8	8.41	5.29	6.29×10^{-4}	0.8	99.97

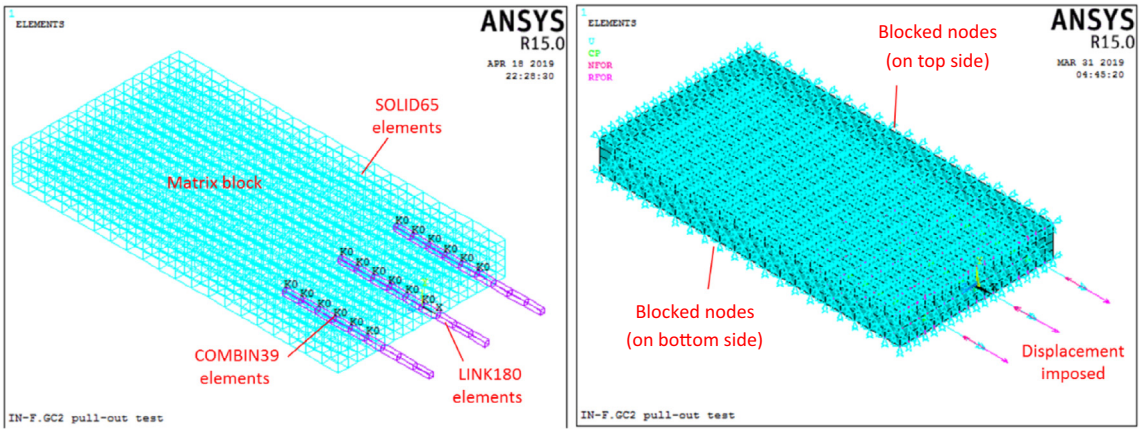

(a) Geometry and meshing (b) Boundary conditions and loading

Fig. 13. Configuration of meshing, boundary conditions and loading for pull-out specimen model.

including the pull-out behaviour of interface specimens, local behaviour of the component materials and specimen failure mode.

4.2.1. Pull-out behaviour of IN-F.GC2 specimens

The pull-out behaviour of IN-F.GC2 specimens with different embedded lengths could be obtained from the numerical model. The pull-out force was calculated from the reaction force at all nodes of textile yarns applied with the displacement imposed, while the slip was the relative displacement between two points at the first position of interface contact, one on matrix block and another one on textile yarn. As numerical results, the interface model showed a trilinear behaviour with four cases of embedded length as input data presented in Fig. 11b. In the first phase, the force increased linearly with the slip between carbon textile and matrix block until the matrix elements around textile yarns were damaged, and the micro-cracks appeared. These micro-cracks were developed and became the tunnel cracks with the increase of the pull-out force. The force decrease appeared when the effective embedded length was reduced because of the damage of matrix elements, and the rest of the interface bond was not strong enough to support the pull-out force. In the last phase, the pull-out force decreased with the increase of textile/matrix slip because the interface model (COMBIN39) was passed in the nonlinear phase.

Concerning the effect of embedded length on pull-out behaviour, the maximum pull-out forceincreased gradually from 1468.4 N to 2606.0 N, corresponding respectively with the extension of embedded length from 2 cm to 4 cm. All values of maximum pull-out force, obtained by numerical modeling, are presented in Table 6 in comparison with those of the experiment. This table also presents other values of pure friction force in the last phase of pull-out behaviour and the percentage errors between both numerical and experimental results. Fig. 14 below presented an agreement between both numerical and experimental results concerning the pull-out behaviour of IN-F.GC2 specimens with different embedded lengths.

4.2.2. Local behaviour of the component materials

In the numerical model for pull-out tests, textile yarns presented a linear behaviour in tensile loading for all elements inside or outside the matrix block. With the displacement imposed at the ends of textile yarns, the stress inthese parts was distributed evenly along the length of the textile yarn. However, for the rest inside the matrix block, the pull-out force was distributed evenly to the matrix elements surrounded by textile/matrix interface elements. This distribution depended on the relative displacement between two points of the nonlinear spring element. So, the stress of textile yarn parts embedded in the matrix block was evolved with the position of the studied point. Fig. 15a, b present respectively the distribution of stress and displacement of all nodes in textile yarns at the calculation step corresponding with the maximum pull-out force for IN-F.GC2 with 2 cm of embedded length.

Concerning the mechanical behaviour of the cementitious matrix in this numerical modeling, the concrete model presented a nonlinear response with the material damage by the element cracks according to three main directions. The first crack of one matrix element appeared in a direction which fitted with the principal direction an angle of 45° because this element was under shear stress state (see micro-cracks in Fig. 17). After the damage of the matrix parts around the textile yarns, it would be pulled out from the matrix block, as shown in Fig. 16b. This numerical result was in good agreement with the observation of the experiment.

4.2.3. Failure mode

The numerical model for all cases of embedded length only showed one failure mode on the pull-out test specimens (see Fig. 17). On the matrix block, the damage of matrix elements could be seen around the textile yarns. These elements (SOLID65) were

Table 6
Comparison of the maximum pull-out force of the experimental and numerical results for IN-F.GC2 specimens.

Results	IN-F.GC2 – 2 cm		IN-F.GC2 – 2.5 cm		IN-F.GC2 – 3 cm		IN-F.GC2 – 4 cm	
	Full-out force (N)	Friction force (N)	Full-out force (N)	Friction force (N)	Full-out force (N)	Friction force (N)	Full-out force (N)	Friction force (N)
Experimental value	1429.79	198.87	1609.71	295.50	2015.29	393.83	2288.29	913.36
Numerical value	1468.38	197.88	1731.72	329.38	2028.41	408.70	2656.02	1145.81
Errors (%)	2.70	0.50	7.58	11.47	0.65	3.78	16.07	25.45

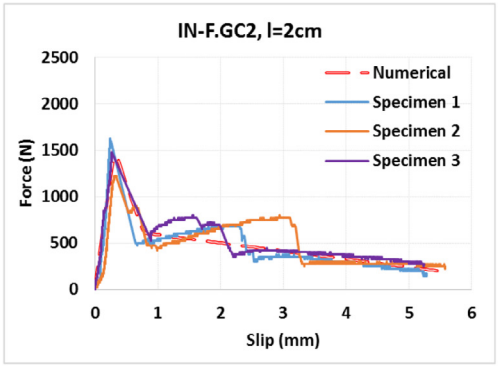

(a) Embedded length of 2 cm

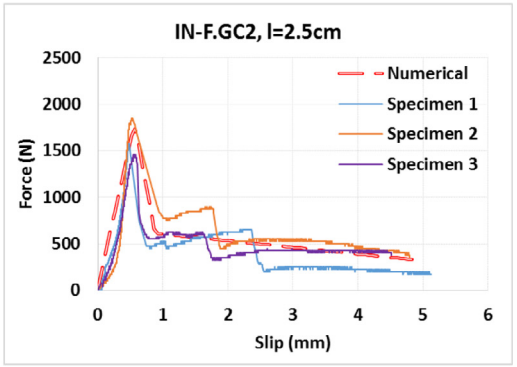

(b) Embedded length of 2.5 cm

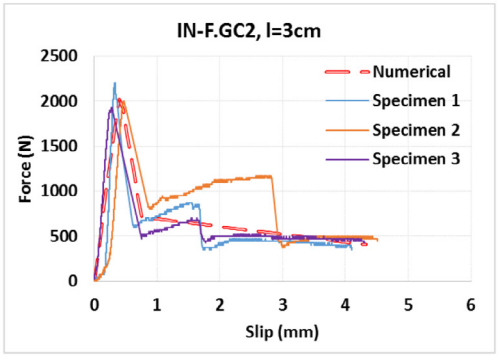

(c) Embedded length of 3 cm

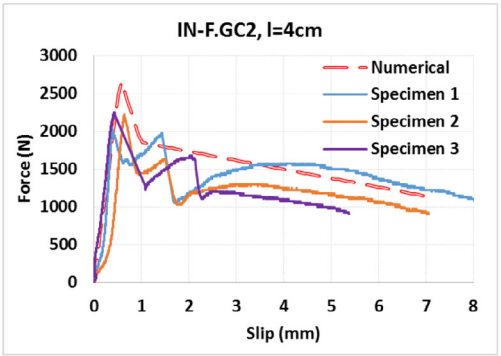

(c) Embedded length of 4 cm

Fig. 14. Comparison of experimental and numerical results on the pull-outbehaviour of IN-F.GC2 specimens with different embedded lengths.

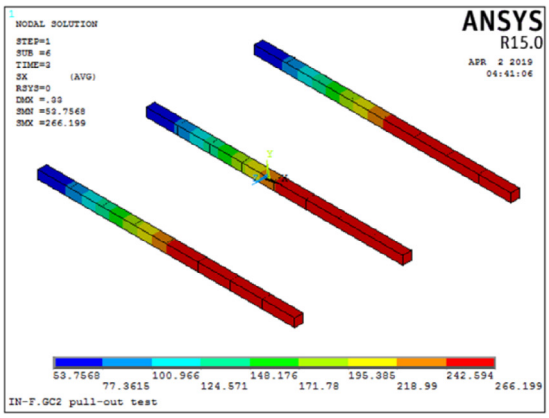

(a) Stress in textile yarns

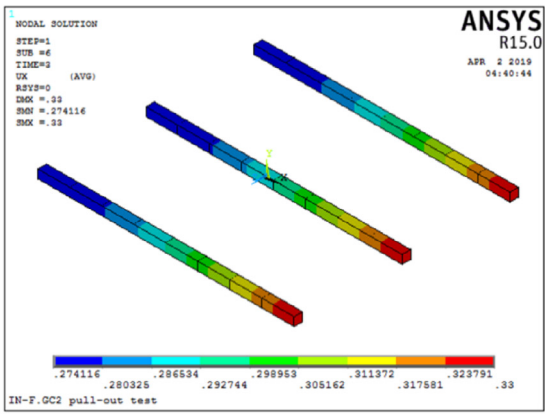

(b) Displacement of all nodes of textile yarns

Fig. 15. Mechanical behaviour of textile yarns at the step of maximum pull-out force for IN-F.GC2 – 2 cm.

directly connected with the elements of textile yarns (LINK180) by the nonlinear spring elements and were strongly deformed under pull-out force action. This shear force also transferred to the other matrix elements around the textile yarn elements (not directly connected) by the shear transfer coefficient of the matrix material model. The numerical model presented the cracks in the matrix elements at positions around textile yarns, as shown in Fig. 17a. The deep of tunnel cracks was generally equal to the slip of pull-out response and was not dependent on the embedded length of carbon textile in the matrix block. However, it could be observed that on pull-out specimens after the numerical calculation, there were several micro-cracks along the embedded length of carbon textile yarns. The number of micro-cracks depended on the embedded length but was not proportional for this dependence.

In comparison with the failure mode of pull-out specimens in the experiment, there was an interesting agreement of the numerical model result. The damage and cracks of the matrix block were presented in the form of conical valleys, as shown in Fig. 17b. Fig. 17 presents the comparison between both experimental and numerical results concerning the failure mode of IN-F.GC2 specimens.

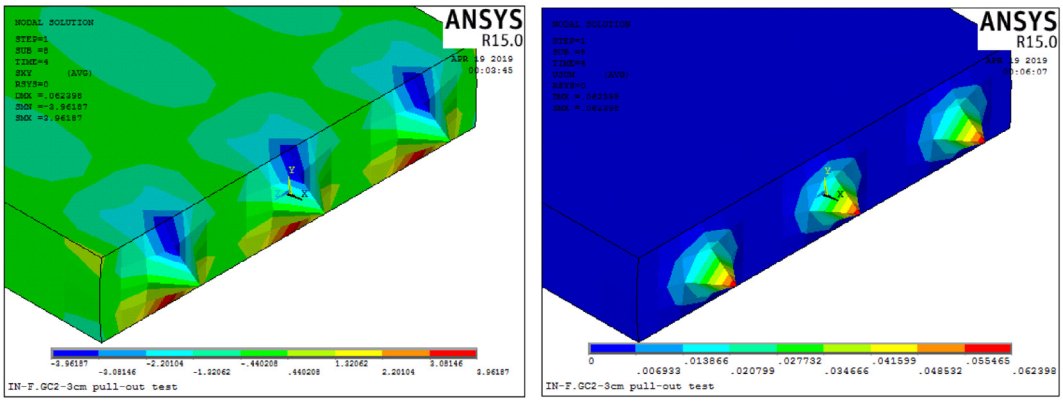

(a) Shear stress of all nodes on matrix block (b) Displacement of all nodes on matrix block

Fig. 16. Mechanical behaviour of cementitious matrix at the step of maximum pull-out force for IN-F.GC2 – 3 cm.

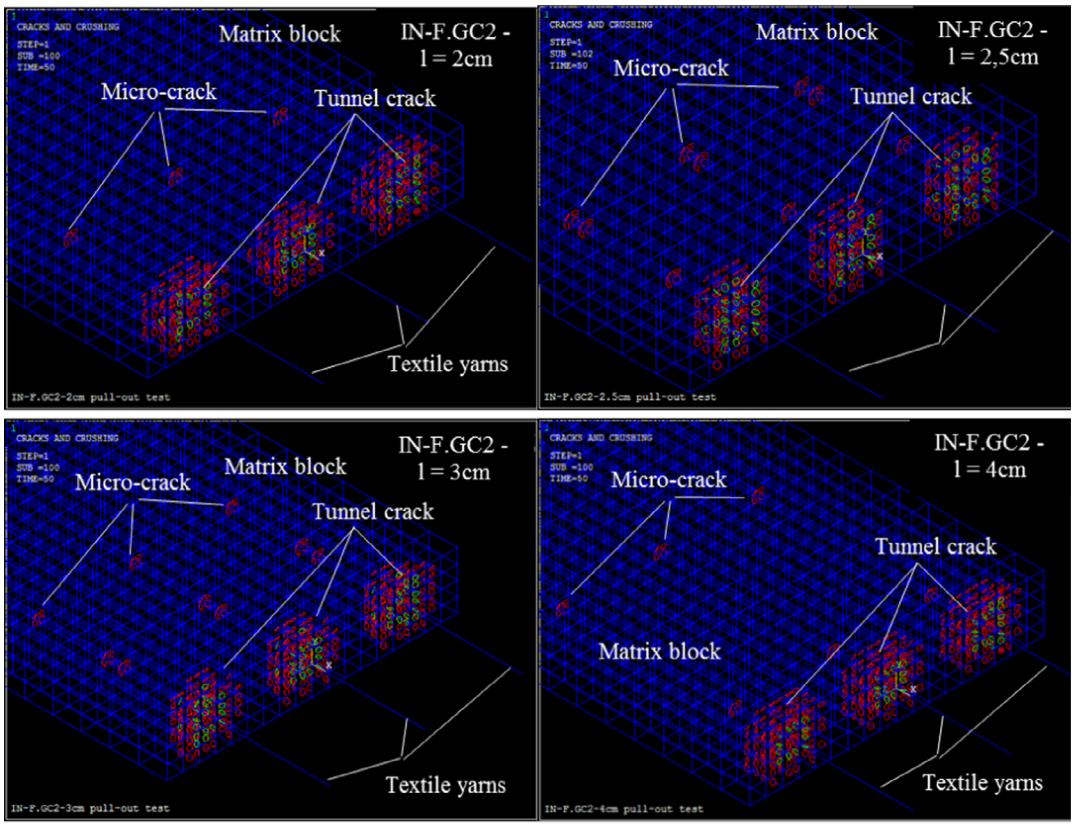

(a) Numerical model

(b) Experimental

Fig. 17. Failure mode of pull-out specimens.

5. Conclusions and future works

This paper presents the experimental and numerical results concerning the behaviour of the interface between GC2 carbon textile and cementitious matrix thanks to the pull-out tests at ambient temperature. Regarding the experimental approach, the pull-out tests were performed on specimens of GC2 textile embedded in a matrix block with different lengths from 2 cm to 4 cm. After that, the numerical model was developed and validated by using a nonlinear spring model for interface behaviour, taking into account the crack damage of the cementitious matrix in the calculation. As both experimental and numerical results obtained, some conclusions following could be drawn for this work:

- The interface behaviour of the carbon textile embedded in the cementitious matrix could be characterized by pull-out tests. The experimental results showed that the textile/matrix interface specimens gave a softening behaviour with three phases as presented in the literature.
- The carbon textile greatly affected the pull-out response of textile/matrix interface. Its geometry under the grid form gave a good connection with the cementitious matrix to hold it back in matrix block, while its treatment product gave a good adherence by generating the thin layer of C-S-H gel around textile yarns. This effect explained the appearance of the tunnel crack and matrix valleys in spiral form.
- The embedded length affected the pull-out behaviour and total pull-out energy of the textile/matrix interface specimens. This was an augmentation in maximal pull-out force, pure friction force, and total energy with the increase of embedded length. However, this tendency was not linear for all cases of embedded length.
- The combination of a nonlinear spring model for textile/matrix interface behaviour, nonlinear behaviour model for cementitious matrix, and linear elastic behaviour for carbon textile gave a reasonable result in comparison with that of the experiment. In this numerical modeling, we also takeinto account the crack damage of the cementitious matrix which indirectly damaged the bond strength of the textile/matrix interface.

For future works, it will be interesting to use the optical fibre to study the textile/matrix interface behaviourof TRC composite, in particular at elevated temperature. After that, it will be also interesting to use the textile/matrix interface model for the numerical modeling of the thermomechanical behaviour of TRC composite material at different temperatures.

Declaration of Competing Interest

The authors declare that they have no known competing financial interests or personal relationships that could have appeared to influence the work reported in this paper.

Acknowledgments

This research has been performed with financial support of LMC2 (thanks to its industrial projects) for the experimental and numerical works, and the financial support of a doctoral scholarship from the Ministry of Education and Training of Vietnam to the first author. We would like to show our gratitude to the society Kerneos Aluminate Technologies, France for supply of materials (cement, aggregates, super-plasticizer). We would also like to express our thanksto the technicians (Mr. E. JANIN, Mr. N. COTTET) from the Civil Engineering Department of IUT Lyon 1 and LMC2, University of Lyon 1 for their technical support.

References

[1] V. Koncar, 1 - Introduction to smart textiles and their applications, in: V. Koncar (Ed.), Smart Textiles and their Applications, Woodhead Publishing, Oxford, 2016, pp. 1–8.
[2] T. Gries, M. Raina, T. Quadflieg, O. Stolyarov, 1 – Manufacturing of textiles for civil engineering applications, in: T. Triantafillou (Ed.), Textile Fibre Composites in Civil Engineering, Woodhead Publishing, 2016, pp. 3–24.
[3] Q.T. Shubhra, A. Alam, M. Quaiyyum, Mechanical properties of polypropylene composites: A review, J. Thermoplast. Compos. Mater. 26 (3) (2013) 362–391.
[4] M. Butler, M. Lieboldt, V. Mechtcherine, Application of textile-reinforced concrete (TRC) for structural strengthening and in prefabrication, in: Proceedings of the International Conference on Advanced Concrete Materials (ACM), Stellenbosch, South Africa, 2010, pp. 125–134.
[5] V. Mechtcherine, Novel cement-based composites for the strengthening and repair of concrete structures, Constr. Build. Mater. 41 (2013) 365–373.
[6] A. Baradaran-Nasiri, M. Nematzadeh, The effect of elevated temperatures on the mechanical properties of concrete with fine recycled refractory brick aggregate and aluminate cement, Constr. Build. Mater. 147 (2017) 865–875.
[7] R. Contamine, A. Si Larbi, P. Hamelin, Contribution to direct tensile testing of textile reinforced concrete (TRC) composites, Mater. Sci. Eng. A, Nov. 528 (29) (2011) 8589–8598.
[8] B. Mobasher, V. Dey, Z. Cohen, A. Peled, Correlation of constitutive response of hybrid textile reinforced concrete from tensile and flexural tests, Cem. Concr. Compos. 53 (2014) 148–161.
[9] C. Soranakom, B. Mobasher, Correlation of tensile and flexural responses of strain softening and strain hardening cement composites, Cem. Concr. Compos. 30 (6) (2008) 465–477.
[10] D.u. Yunxing, M. Zhang, F. Zhou, D. Zhu, Experimental study on basalt textile reinforced concrete under uniaxial tensile loading, Constr. Build. Mater. 138 (2017) 88–100.
[11] R. Contamine, A. Junes, A. Si Larbi, Tensile and in-plane shear behaviour of textile reinforced concrete: analysis of a new multiscale reinforcement, Constr. Build. Mater. 51 (2014) 405–413.
[12] A. Peled, Bonds in textile-reinforced concrete composites, Text. Fibre Compos. Civ. Eng., pp. 63–99, Jan. 2016.
[13] A. Peled, A. Bentur, D. Yankelevsky, Effects of woven fabric geometry on the bonding performance of cementitious composites: mechanical performance, Adv. Cem. Based Mater. 7 (1) (1998) 20–27.
[14] R. Barhum, V. Mechtcherine, Effect of short, dispersed glass and carbon fibres on the behaviour of textile-reinforced concrete under tensile loading, Eng. Fract. Mech. 92 (2012) 56–71.
[15] J. Donnini, G. Lancioni, V. Corinaldesi, Failure modes in FRCM systems with dry and pre-impregnated carbon yarns: experiments and modeling, Compos. Part B Eng. 140 (2018) 57–67.
[16] S. L. Gao, E. Mäder, R. Plonka, Coatings for Fibre and Interphase Modification in a Cementitious Matrix., Report of Leibniz Institute of Polymer Research Dresden (IPF).
[17] F. Teklal, A. Djebbar, S. Allaoui, G. Hivet, Y. Joliff, B. Kacimi, A review of analytical models to describe pull-out behavior – fiber/matrix adhesion, Compos. Struct. 201 (2018) 791–815.
[18] O. Homoro, M. Michel, T.N. Baranger, Pull-out response of glass yarn from ettringite matrix: effect of pre-impregnation and embedded length, Compos. Sci. Technol. 170 (2019) 174–182.
[19] S.R. Ferreira, E. Martinelli, M. Pepe, F. de Andrade Silva, R.D. Toledo Filho, Inverse identification of the bond behavior for jute fibers in cementitious matrix, Compos. Part B Eng., Jun. 95 (2016) 440–452.
[20] S.R. Ferreira, M. Pepe, E. Martinelli, F. de Andrade Silva, and R. D. Toledo Filho, "Influence of natural fibers characteristics on the interface mechanics with cement based matrices," Compos. Part B Eng., vol. 140, pp. 183–196, May 2018.
[21] X.B. Zhang, H. Aljewifi, J. Li, Failure mechanism investigation of continuous fibre reinforced cementitious composites by pull-out behaviour analysis, Procedia Mater. Sci. 3 (2014) 1377–1382.
[22] X.B. Zhang, H. Aljewifi, J. Li, Failure behaviour investigation of continuous yarn reinforced cementitious composites, Constr. Build. Mater. 47 (2013) 456–464.
[23] F. de A. Silva, M. Butler, S. Hempel, R.D. Toledo Filho, V. Mechtcherine, Effects of elevated temperatures on the interface properties of carbon textile-reinforced concrete, Cem. Concr. Compos., Apr. 48 (2014) 26–34.
[24] M. Butler, V. Mechtcherine, S. Hempel, Experimental investigations on the durability of fibre–matrix interfaces in textile-reinforced concrete, Cem. Concr. Compos. 31 (4) (2009) 221–231.
[25] M.E.A. Fidelis, R.D. Toledo Filho, F. de A. Silva, V. Mechtcherine, M. Butler, S. Hempel, The effect of accelerated aging on the interface of jute textile reinforced concrete, Cem. Concr. Compos., Nov. 74 (2016) 7–15.
[26] S.R. Ferreira, F. de A. Silva, P.R.L. Lima, R.D. Toledo Filho, Effect of fiber treatments on the sisal fiber properties and fiber–matrix bond in cement based systems, Constr. Build. Mater., Dec. 101 (2015) 730–740.
[27] M. Lu, H. Xiao, M. Liu, X. Li, H. Li, L. Sun, Improved interfacial strength of SiO2 coated carbon fiber in cement matrix, Cem. Concr. Compos. 91 (Aug. 2018) 21–28.
[28] W. Zhang, X. Xu, H. Wang, F. Wei, Y. Zhang, Experimental and numerical analysis of interfacial bonding strength of polyoxymethylene reinforced cement composites, Constr. Build. Mater. 207 (2019) 1–9.

[29] S. Zhandarov, E. Mäder, Characterization of fiber/matrix interface strength: applicability of different tests, approaches and parameters, Compos. Sci. Technol. 65 (1) (2005) 149–160.
[30] C. Baley, Y. Grohens, F. Busnel, P. Davies, Application of interlaminar tests to marine composites. relation between glass fibre/polymer interfaces and interlaminar properties of marine composites, Appl. Compos. Mater. 11 (2) (2004) 77–98.
[31] A. Dalalbashi, B. Ghiassi, D.V. Oliveira, A. Freitas, Fiber-to-mortar bond behavior in TRM composites: effect of embedded length and fiber configuration, Compos. Part B Eng. 152 (2018) 43–57.
[32] G. Ferrara, M. Pepe, E. Martinelli, R. Dias Tolêdo Filho, Influence of an Impregnation Treatment on the Morphology and Mechanical Behaviour of Flax Yarns Embedded in Hydraulic Lime Mortar, Fibers, vol. 7, no. 4, p. 30, Apr. 2019.
[33] E. Grande, G. Milani, Interface modeling approach for the study of the bond behavior of FRCM strengthening systems, Compos. Part B Eng. 141 (2018) 221–233.
[34] E. Grande, M. Imbimbo, E. Sacco, Numerical investigation on the bond behavior of FRCM strengthening systems, Compos. Part B Eng. 145 (2018) 240–251.
[35] F.G. Carozzi, P. Colombi, G. Fava, C. Poggi, A cohesive interface crack model for the matrix–textile debonding in FRCM composites, Compos. Struct. 143 (2016) 230–241.
[36] Z.I. Djamai, M. Bahrar, F. Salvatore, A. Si Larbi, M. El Mankibi, Textile reinforced concrete multiscale mechanical modelling: application to TRC sandwich panels, Finite Elem. Anal. Des., Nov. 135 (2017) 22–35.
[37] A. Dalalbashi, B. Ghiassi, D.V. Oliveira, A. Freitas, Effect of test setup on the fiber-to-mortar pull-out response in TRM composites: experimental and analytical modeling, Compos. Part B Eng. 143 (2018) 250–268.
[38] G. Mazzucco, T. D'Antino, C. Pellegrino, V. Salomoni, Three-dimensional finite element modeling of inorganic-matrix composite materials using a mesoscale approach, Compos. Part B Eng. 143 (2018) 75–85.
[39] M.T. Tran, X.H. Vu, E. Ferrier, Mesoscale experimental investigation of thermomechanical behaviour of the carbon textile reinforced refractory concrete under simultaneous mechanical loading and elevated temperature, Constr. Build. Mater. 217 (2019) 156–171.
[40] European standard BS EN 196-1, Methods of testing cement. Determination of strength, s.l.: s.n., 2005.
[41] ANSYS, Theory reference for the mechanical APDL and Mechanical Applications, ANSYS Inc, 2009, edited by P, Kohnke.
[42] ANSYS, Mechanical APDL Element Reference, ANSYS Inc, Release 14, 2011.
[43] M.T. Tran, X.H. Vu, E. Ferrier, Experimental and analytical analysis of the effect of fibre treatment on the thermomechanical behaviour of continuous carbon textile subjected to simultaneous elevated temperature and uniaxial tensile loadings, Constr. Build. Mater. 183 (2018) 32–45.